Inhibition of spikes in an array of coupled FitzHugh–Nagumo oscillators by means of alternating current

Arūnas Tamaševičius, Gytis Mykolaitis, Elena Adomaitienė, and Skaidra Bumelienė

***Abstract*—**Damping of spikes in an array of coupled oscillators by injection of sinusoidal current is studied both experimentally and numerically. The effect is investigated using an array, consisting of thirty mean-field coupled FitzHugh–Nagumo type oscillators. The results are considered as a possible mechanism of the deep brain stimulation, used to avoid the symptoms of the Parkinson's disease.

***Keywords*—**Alternating current, arrays of coupled oscillators, control of oscillations, FitzHugh–Nagumo oscillators.

I. Introduction

Undesirable instabilities in dynamical systems can be avoided by applying conventional proportional feedback techniques [1, 2]. An example is a simple second order system, where the proportional feedback is given by a linear term with a control coefficient k:

$$\begin{aligned} \dot{x} &= F(x, y) + k(x^* - x), \\ \dot{y} &= G(x, y). \end{aligned} \tag{1}$$

Here $F(\cdot)$ and $G(\cdot)$ are either linear or nonlinear functions, the x^* is a reference point, e.g. a steady state coordinate of the system. However, in many real systems, especially in biology, chemistry, physiology, etc., the exact locations of these states are unknown. Moreover, their positions may vary with time because of unknown and unpredictable forces. Therefore adaptive methods, automatically tracing and stabilizing the steady states are required. A large number of adaptive control techniques have been developed so far, e.g. the tracking filter method [3, 4], and applied to a variety of dynamical systems. To implement the tracking filter technique (1) should be provided with an additional equation, describing the dynamical variable z of the first order filter:

$$\begin{aligned} \dot{x} &= F(x, y) + k(z - x), \\ \dot{y} &= G(x, y), \\ \dot{z} &= \omega_f (x - z), \end{aligned} \tag{2}$$

where ω_f is the cut-off frequency of the filter (usually $\omega_f << 1$).

An alternative control method is a non-feedback technique based on applying to the system external periodic force:

$$\begin{aligned} \dot{x} &= F(x, y) + A\sin(\omega t), \\ \dot{y} &= G(x, y). \end{aligned} \tag{3}$$

In (3) the frequency of the external forcing ω should be high enough in comparison of the natural frequency of the uncontrolled dynamical system. A specific example is the stabilization of the unstable upside-down position of a mechanical pendulum by vibrating its pivot up and down at a relatively high frequency [5]. Recently [6] this "mechanical" idea has been exploited in a seemingly unexpected field, namely to get insight into the mechanism of the so-called deep brain stimulation (DBS), conventionally used to avoid tremor for patients with the Parkinson's disease.

In this paper, we extend this research by demonstrating that external periodic forcing can inhibit spikes in an array of coupled neuronal oscillators. To be specific, we consider an array of the mean-field coupled electronic FitzHugh–Nagumo (FHN) oscillators, also known in literature as the Bonhoeffer–van der Pol oscillators.

II. Electrical Circuits

The corresponding circuit diagrams are presented in Fig. 1. In Fig. 1(a) CN is a coupling node. It is assumed, that the CN is not accessible directly from the outside, but via some passive resistance network, represented here for simplicity by an equivalent resistance R_g. DN is an accessible damping node.

In Fig. 1(b) OA is a general-purpose operational amplifier, e.g. NE5534 type device, D_1 and D_2 are the BAV99 type Schottky diodes, $L = 10$ mH, $C = 3.3$ nF, $R_1 = R_2 = 1$ kΩ, $R_3 = 510$ Ω, $R_4 = 30$ Ω, $R_5 = 510$ Ω, $R_6 = 275$ Ω (an external resistor $R_6' = 220$ Ω in series with the coil resistance $R_6'' = 55$ Ω), $R_{7i} = (24+i)$ kΩ, $i = 1, 2, \ldots N$, $R^* = 510$ Ω, $V_0 = -15$ V.

A. Tamaševičius (corresponding author, phone: 370-671-93904; fax: 370-5-262-7123; e-mail: tamasev@pfi.lt), E. Adomaitienė (e-mail: elena.tamaseviciute@ftmc.lt), and S. Bumelienė (e-mail: skaidra@pfi.lt) are with the Department of Electronics, Center for Physical Sciences and Technology, 11 A. Goštauto str., LT-01108 Vilnius, Lithuania.

G. Mykolaitis is with the Department of Physics, Faculty of Fundamental Sciences, Vilnius Gediminas Technical University, 11 Saulėtekio al., LT-10223 Vilnius, Lithuania (e-mail: gytis@pfi.lt).

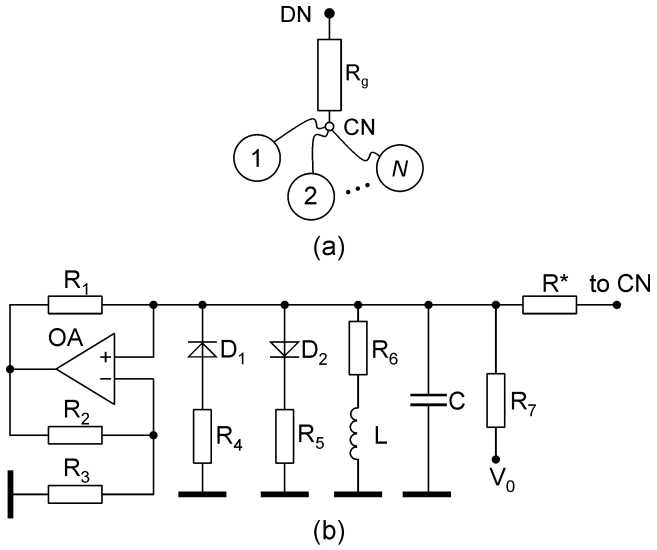

Fig. 1 Circuit diagrams. (a) array of mean-field coupled oscillators, (b) single asymmetric ($R_4 << R_5$) FHN type oscillator

The single FHN oscillator in Fig. 1(b) is a circuit with an *asymmetric* nonlinearity ($R_4 << R_5$). It is a slight modification of an oscillator, described in [7] and essentially differs from the earlier asymmetric version of the FHN type oscillator, suggested in [8].

In the experiments we employed a hardware array with $N = 30$, described in details (without any external control) elsewhere [9].

III. Experimental Results

The external inhibitory AC current $I_{inh}(t) = I_A \sin(2\pi f t)$ was injected from an external sine wave generator via the damping node DN. For the best performance it is necessary to choose an appropriate drive amplitude I_A and frequency f. The f should be much higher than the natural frequency f_0 of the spiking oscillators ($f_0 \approx 12$ kHz). The experimental results are shown in Fig. 2 and Fig. 3, by the waveforms and the phase portraits (in classical electronics called the Lissajous figures). Here the $<V_C>$ is the mean-field voltage of the voltages V_{Ci} from the individual oscillators ($i = 1, 2 \ldots 30$). The threshold amplitude of the inhibitory current is $I^*_A = 50$ mA, the optimal frequency is $f \approx 150$ kHz, providing the lowest threshold.

The time average of the high frequency non-spiking voltage $<V_C>$ (right hand side of the bottom plot), taken over the period ($T = 1/f$) of the external current, is $\bar{U}_C \approx -0.18$ V. It is non-zero value because of the DC bias $V_0 = -15$ V. The $\bar{U}_C$ is noticeably different from the natural steady state $<V_{0C}> = -0.27$ V, measured in a non-oscillatory mode (when the all coils L are short-circuited).

Fine diagonals in Fig. 3, $[V_{C30}, <V_C>]$ indicate, that the individual oscillator #30 is strongly synchronized with the mean-field of the array. Other oscillators, #1 to #29 were also checked experimentally by means of the phase portraits $[V_{Ci}, <V_C>]$ and gave similar result.

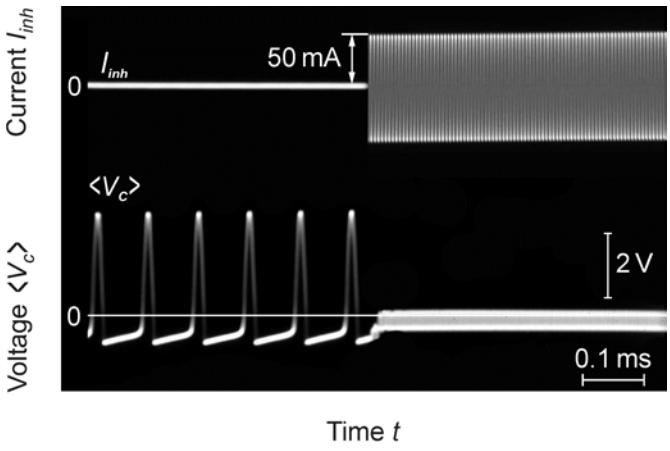

Fig. 2 Experimental waveforms of the external periodic current I_{inh} and the mean-field voltage of the array $<V_C>$. $f = 150$ kHz

Evidently, the self-sustained low frequency ($f_0 \approx 12$ kHz) spikes of about 4 V height are totally suppressed, when the inhibitory current $I_A \geq I_A^* = 50$ mA is injected. However, we have a finite (≈ 10%) higher frequency artefact. The voltage oscillates around the time average $\bar{U}_C$ with the amplitude of about 0.4 V at the external drive frequency f.

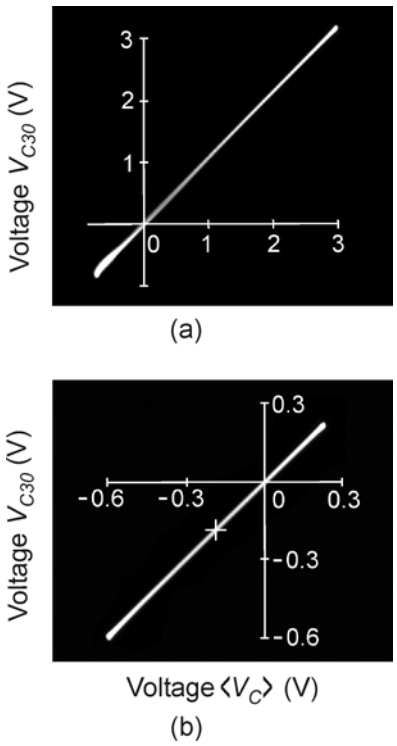

Fig. 3 Phase portraits $[V_{C30}, <V_C>]$. (a) Spiking oscillators (no control, $I_A = 0$), (b) Non-spiking oscillators, $I_A = 50$ mA, $f = 150$ kHz. Small cross in (b) marks the averages of the voltages $[\bar{U}_{C30}, \bar{U}_C]$ taken over the period of the external inhibitory current $I_{inh}(t)$. They are at about [–0.18 V, –0.18 V]. Note different position of the diagonal also different horizontal and vertical scales in (b), compared to (a)

Moreover, the artefact voltage continues to change (Fig. 4), when the external drive amplitude I_A is increased above the threshold value I^*_A (the amplitude I_A should be somewhat higher than the threshold to guarantee robust inhibition). For example, at a double drive amplitude, $I_A/I_A^* = 2$ the average voltage changes its sign. Similar behavior was observed earlier, but not emphasized, in the numerically simulated bifurcation diagram for the Hodgkin–Huxley (HH) single neuron model [6].

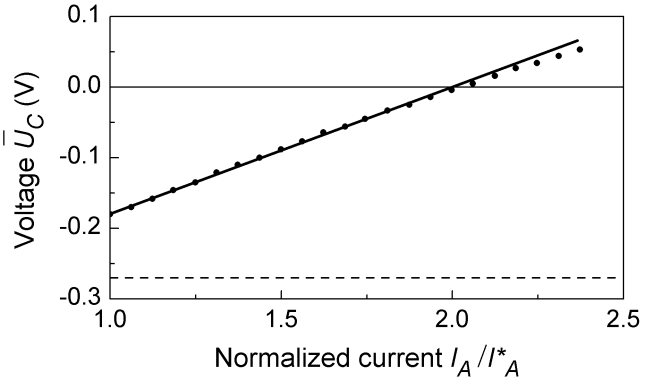

Fig. 4 Time average of the mean-field voltage $\bar{U}_C$, taken over the period ($T = 1/f$) of the external inhibitory current I_{inh}, as a function of the normalized amplitude I_A/I_A^* of the external current. $I_A^* = 50$ mA. Extrapolation to zero control ($I_A = 0$) provides a value of $\bar{U}_C$ close to the natural steady state $\langle V_{0C} \rangle = -0.27$ V (dashed line in the plot)

IV. Mathematical Model

Applying the Kirchhoff's laws to the circuits in Fig. 1 with $R_1 = R_2$ and $R_7 >> \max((L/C)^{1/2}, R_3, R_4, R_5, R_6)$ the following differential equations are derived:

$$\begin{aligned} C\frac{dV_{Ci}}{dt} &= \frac{V_{Ci}}{R_3} - I_D - I_{Li} + \frac{V_0}{R_{7i}} + \frac{\langle V_C \rangle - V_{Ci}}{R^*} + \frac{I_A \sin(2\pi f t)}{N}, \\ L\frac{dI_{Li}}{dt} &= V_{Ci} - R_6 I_{Li}, \quad i = 1, 2 \ldots N. \end{aligned} \tag{4}$$

The nonlinear current-voltage (I-V) characteristic $I_D = I_D(V_{Ci})$ of the D_1R_4–D_2R_5 composite in (4) is approximated by three segments of linear functions

$$I_D(V_{Ci}) = \begin{cases} (V_{Ci} + V^*)/R_4 & , \quad V_{Ci} < -V^*, \\ 0 & , \quad -V^* \le V_{Ci} \le V^*, \\ (V_{Ci} - V^*)/R_5 & , \quad V_{Ci} > V^*. \end{cases} \tag{5}$$

Here V^* is the "breakpoint" voltage of the forward I-V characteristic of the diodes ($V^* \approx 0.6$ V). In (4) the individual oscillators are coupled via the mean-field voltage

$$\langle V_C \rangle = \frac{1}{N}\sum_{i=1}^{N} V_{Ci} \, . \tag{6}$$

By introducing the following set of dimensionless variables and parameters:

$$\begin{gathered} x_i = \frac{V_{Ci}}{V^*}, \quad y_i = \frac{\rho I_{Li}}{V^*}, \quad t \to \frac{t}{\sqrt{LC}}, \\ \langle x \rangle = \frac{1}{N}\sum_{i=1}^{N} x_i, \quad \rho = \sqrt{L/C}, \\ a = \frac{\rho}{R_3}, \quad b = \frac{R_6}{\rho}, \quad c_i = \frac{\rho}{R_{7i}} \cdot \frac{V_0}{V^*}, \\ d_1 = \frac{\rho}{R_4}, \quad d_2 = \frac{\rho}{R_5}, \quad k = \frac{\rho}{R^*}, \quad i = 1, 2, \ldots N \end{gathered} \tag{7}$$

also two additional dimensionless parameters for the external sine wave forcing:

$$A = \frac{\rho I_A}{N V^*}, \quad \omega = 2\pi f \sqrt{LC} \tag{8}$$

we arrive to a set of $2N$ coupled non-autonomous differential equations, convenient for numerical integration:

$$\begin{aligned} \dot{x}_i &= a x_i - f(x_i) - y_i + c_i + k(\langle x \rangle - x_i) + A \sin \omega t, \\ \dot{y}_i &= x_i - b y_i, \quad i = 1, 2, \ldots N. \end{aligned} \tag{9}$$

The $f(x_i)$ in (9) is a nonlinear function, presented by a piecewise linear function

$$f(x_i) = \begin{cases} d_1(x_i + 1) & , \quad x_i < -1, \\ 0 & , \quad -1 \le x_i \le 1, \\ d_2(x_i - 1) & , \quad x_i > 1. \end{cases} \tag{10}$$

Note, that due to $d_1 >> d_2$ the $f(x_i)$ is an essentially asymmetric function [7] in contrast to the common FHN cubic parabola x^3, introduced by FitzHugh [10]. The DC bias parameters c_i are intentionally set different for each individual oscillator, thus making them non-identical units.

V. Numerical Results

Integration of (9) has been performed using the Wolfram MATHEMATICA package. The numerical results are presented in Fig. 5. They are in a good agreement with the experimental plots in Fig. 2. The mean-field variable $\langle x_i \rangle$ does not converge to a constant steady state, but oscillates around it at the drive frequency. Strictly speaking, the non-autonomous (externally driven) dynamical systems, e.g. given by (9), do not possess steady states at all. Only in the case of high frequency ($f >> f_0$) drive we can introduce the average values, taken over the external period. These averages more or less are related to the steady states.

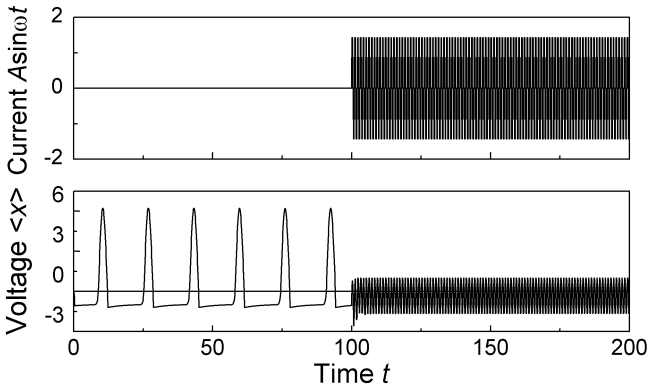

Fig. 5 Simulated waveforms of the inhibitory current $A\sin(\omega t)$ and the mean-field voltage $\langle x \rangle$ from (9, 10), $N = 30$. $A = 5.1$, $\omega = 6.28$, $a = 3.4$, $b = 0.16$, $c_i = -44/(24 + i)$, $i = 1, 2, \ldots 30$, $d_1 = 60$, $d_2 = 3.4$, $k = 3.4$. The external inhibitory term $A\sin(\omega t)$ is activated at $t = 100$

VI. Mean-Field Approach and Linear Analysis

Analysis of (9) can be essentially simplified, if we consider the mean-field variables only, obtained by direct averaging the x_i, y_i, $f(x_i)$, and c_i in the original equations:

$$\begin{aligned} \langle \dot{x} \rangle &= a\langle x \rangle - \langle f(x) \rangle + \langle y \rangle + \langle c \rangle + A\sin \omega t, \\ \langle \dot{y} \rangle &= \langle x \rangle - b\langle y \rangle. \end{aligned} \tag{11}$$

As a result, the coupling term $k(\ldots)$ in (11) has been nullified independently on the value of k. Further we assume, that all $|x_i| \le 1$. According to (10) this leads to $f(x_i) = 0$. Eventually we obtain a set of linear differential equations, which does not describe the full dynamics of the mean field, but provides its steady state. In the absence of the external drive ($A = 0$) it has the following coordinates (for $ab < 1$ and $|c_i| \le 1/b - a$):

$$\langle x_0 \rangle = b\langle c \rangle / (1 - ab), \quad \langle y_0 \rangle = \langle c \rangle / (1 - ab). \tag{12}$$

Stability analysis of (11) shows, that for and $a > b$ the steady state, given by (12), is unstable (the real parts of the both eigenvalues of the corresponding second order characteristic equation are both positive). If (in addition to $a > b$) the sum $a + b > 2$, then the eigenvalues are real (no imaginary parts). Thus, the steady state (12) is an unstable node. Whereas the external periodic forcing ($A \ne 0$), similarly to the mechanical pendulum [5], can stabilize the originally unstable steady state.

For the set of the parameter values, employed in numerical simulations: $a = 3.4$, $b = 0.16$, and $c_i = -44/(24+i)$, the steady-state coordinates, given by (12), have the following numerical values: $\langle x_0 \rangle = -0.41$, $\langle y_0 \rangle = -2.57$. Using the definitions of the dimensionless variables, introduced in (7), we estimate the means of the steady-state coordinates of the original system: $\langle V_{0C} \rangle \approx -0.25\,\mathrm{V}$, $\langle I_{0L} \rangle \approx -1\,\mathrm{mA}$. The estimated steady-state voltage is close to its experimental value –0.27 V.

VII. Conclusion

In the recent theoretical papers on suppression of neuronal spikes by means of alternating current, the mathematical models of *single* neurons have been considered, the HH [6] and the FHN [11] models, respectively. Our earlier paper [7] on the adaptive feedback technique, suggested to damp spiking FHN type neurons also deals with a *single* oscillator only. In contrast to the above papers, in the present work we have investigated an *array* of coupled FHN type neuronal oscillators. Moreover, using an analogue electronic network we have carried out an imitative experiment. It can serve for better understanding the DBS technique, used to suppress the symptoms of the Parkinson's disease.

The influence of the strongly perturbed steady states of the neurons on the treatment by means of the DBS technique [12] has not been investigated yet. However, one can intuitively suppose, that the high frequency artefact oscillations, observed in the "electronic" experiment (Fig. 2) due to injection of the alternating current into an array of oscillators and especially its unnatural DC component (Fig. 4) can indicate the reason of undesirable side effects in the real neuronal cells.

References

[1] B. C. Kuo, *Automatic Control Systems*. Englewood Cliffs, New Jersey: Prentice Hall, 1995.

[2] K. Ogata, *Modern Control Engineering*. Englewood Cliffs, New Jersey: Prentice Hall, 2010.

[3] N. F. Rulkov, L. S. Tsimring, and H. D. I. Abarbanel, "Tracking unstable orbits in chaos using dissipative feedback control," *Phys. Rev. E*, vol. 50, pp. 314-324, 1994.

[4] A. Namajūnas, K. Pyragas, and A. Tamaševičius, "Analog techniques for modeling and controlling the Mackey–Glass system," *Int. J. Bifurcation Chaos*, vol. 7, no.4, pp. 957–962, 1997.

[5] J. J. Thomsen, Vibrations and Stability – Advanced Theory, Analysis and Tools. Berlin, Heidelberg, New York: Springer-Verlag, 2003.

[6] K. Pyragas, V. Novičenko, and P. A. Tass, "Mechanism of suppression sustained neuronal spiking under high-frequency stimulation," *Biol. Cybern.*, vol. 107, pp. 669-684, 2013.

[7] A. Tamaševičius, E. Tamaševičiūtė, G. Mykolaitis, S. Bumelienė, R. Kirvaitis, and R. Stoop, "Neural spike suppression by adaptive control of an unknown steady state," in *Proc. 19th Int. Conf. Artificial Neural Networks*, Limassol, Cyprus, September 2009; *Lecture Notes Comp. Sci.*, vol. 5768, pp. 618–627, 2009.

[8] S. Binczak, V. B. Kazantsev, V. I. Nekorkin, and J. M. Bilbaut, "Experimental study of bifurcations in modified FitzHugh-Nagumo cell," *Electron. Lett.*, vol. 39, no. 13, pp. 961–962, 2003.

[9] E. Tamaševičiūtė, G. Mykolaitis, and A. Tamaševičius, "Analogue modelling an array of the FitzHugh–Nagumo oscillators," *Nonlinear Analysis: Modelling and Control*, 2012, vol 17, no. 1, pp. 118–125, 2012. Available: http://www.mii.lt/na

[10] R. FitzHugh, "Impulses and physiological states in theoretical models of nerve membrane," *Biophys. J.*, vol. 1, no. 6, pp. 445–466, 1961.

[11] A. Rabinovitch, Y. Biton, D. Braunstein, M. Friedman, and I. Aviram, "A neuron under external sinusoidal stimulation," *Brain Stimul.*, vol. 8, pp. 310-325, 2015.

[12] A. L. Benabid, S. Chabardes, J. Mitrofanis, and P. Polak, "Deep brain stimulation of the subthalamic nucleus for the treatment of Parkinson's disease," *Lancet Neurol.*, vol. 8, no. 1, pp. 67–81, 2009.